Accepted Manuscript

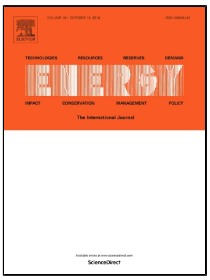

Optimisation of high-temperature heat pump cascades with internal heat exchangers using refrigerants with low global warming potential

Adrián Mota-Babiloni, Carlos Mateu-Royo, Joaquín Navarro-Esbrí, Francisco Molés, Marta Amat-Albuixech, Ángel Barragán Cervera

PII:	S0360-5442(18)31960-1
DOI:	10.1016/j.energy.2018.09.188
Reference:	EGY 13882
To appear in:	*Energy*
Received Date:	06 June 2018
Accepted Date:	28 September 2018

Please cite this article as: Adrián Mota-Babiloni, Carlos Mateu-Royo, Joaquín Navarro-Esbrí, Francisco Molés, Marta Amat-Albuixech, Ángel Barragán Cervera, Optimisation of high-temperature heat pump cascades with internal heat exchangers using refrigerants with low global warming potential, *Energy* (2018), doi: 10.1016/j.energy.2018.09.188

Optimisation of high-temperature heat pump cascades with internal heat exchangers using refrigerants with low global warming potential

Adrián Mota-Babiloni[1], Carlos Mateu-Royo, Joaquín Navarro-Esbrí, Francisco Molés, Marta Amat-Albuixech, Ángel Barragán Cervera

ISTENER Research Group, Department of Mechanical Engineering and Construction, Universitat Jaume I, Campus de Riu Sec s/n, E12071 Castellón de la Plana, Spain

Abstract

High-temperature heat pumps (HTHPs) based on vapour compression can be used for industrial low-grade waste heat valorisation, which can aid in mitigating climate change. Currently, the performance of HTHPs operating at high-temperatures lifts is limited; therefore, advanced configurations become an opportunity for their utilization. This paper presents an HTHP cascade with configurations of internal heat exchangers (IHXs) that uses low GWP refrigerants in both high-stage (HS) (HCFO-1233zd(E), HFO-1336mzz(Z), HCFO-1224yd(Z), and pentane) and low-stage (LS) (HFO-1234yf, HFO-1234ze(E), butane, isobutane, and propane) cycles. Prior to the analysis and presentation of results, an optimisation of the operating conditions is performed based on intermediate temperature and IHX effectiveness in both stage cycles. Results indicate that butane and isobutane appear to be the most convenient working LS fluids from the point of view of coefficient of performance (COP). The highest system performance is obtained using pentane and HFO-1336mzz(Z) in the HS cycle. Compared to third-generation refrigerants (HFC-245fa/HFC-134a), a slight COP improvement is obtained using HCFO-1233zd(E), and HCFO-1224yd(Z). A comparable or even lower volumetric flow rate at the HS compression suction is also observed. The use of pentane/butane achieved maximum COP (3.15), which is a 13% improvement compared to COP obtained when HFC-245fa/HFC-134a is employed.

Highlights

- A high-temperature heat pump cascade with the IHXs is proposed and optimised.
- Synthetic and natural refrigerants with low GWPs are proposed for both stages.
- The higher effectiveness of both IHXs in similar proportions increases total COP.
- Pentane/butane presents maximum COP and minimum HCFO-1224yd(Z)/HFO-1234yf.
- A few refrigerant pairs are comparable with HFC-245fa/HFC-134a in the stages of $\dot{V}_{suc}$.

Keywords: low-grade waste heat recovery; hydrofluoroolefin (HFO); liquid-to-suction heat exchanger; energy efficiency; vapour compression system; climate change mitigation

Nomenclature

a, b, k_e, k_s, k_1, k_2	Pierre's correlation constants [1]
$c_{p,l}$	specific heat of saturated liquid refrigerant (kJ kg^{-1} K^{-1})

[1] Corresponding author: Adrián Mota Babiloni
E-mail: mota@uji.es

COP	coefficient of performance (-)
h	enthalpy (kJ kg^{-1})
Δh_{vap}	latent heat of vaporization (kJ kg^{-1})
$\dot{m}$	refrigerant mass flow rate (kg s^{-1})
P	pressure (MPa)
$\dot{Q}$	heat transfer (kW)
T	temperature (°C)
$\dot{V}$	volumetric flow rate (m^3 s^{-1})
$\dot{W}$	electric power consumption (kW)
Greek symbols	
ε	effectiveness (-)
η	efficiency (-)
ρ	density (kg m^{-3})
Subscripts	
c	compressor
cond	condensation
crit	critical
em	electromechanical
evap	evaporation
I	intermediate
in	inlet
is	isentropic
k	condenser
o	evaporator
out	outlet
suc	suction
vol	volumetric
x	expansion device
Abbreviations	
GWP	global warming potential
HCFO	hydrochlorofluoroolefin
HFC	hydrofluorocarbon
HFO	hydrofluoroolefin
HS	high-stage
HTHP	high-temperature heat pump
IHX	internal heat exchanger
LS	low-stage

1. Introduction

The waste heat potential of European industries accounts for 370.41 TWh [2]. Heat pumps based on vapour compression systems can increase the thermal degree through electricity consumption. On the other hand, heat from sewage water, ambient water resources, and industrial excess heat, among others, have been considered as primary heat sources for heat pumps[3]. Furthermore, the results obtained by Seck et al. [4] showed that heat pumps could be a promising energy recovery technology for the food and beverage industries.

High-temperature heat pumps (HTHPs) can recover heat in the range 60–120 °C and increase it to temperatures 80–160 °C. Therefore, these systems can operate at higher temperatures compared

with those of the usual heat pumps employed for domestic heating and hot water production [5]. The HTHP design and performance are sensitive to the typically wide operating range (high-temperature lift). Based on experimental and numerical investigations, Chamoun et al. [6] reported that the HTHP performance highly depends on the available waste heat and supply process temperatures. Zhao et al. [7] showed that the increase in heating temperature decreases the system's coefficient of performance (COP) and simultaneously increases the compressor's discharge temperature.

Consequently, high-temperature lifts present in the HTHP can lead to a higher energy consumption because of the increase in the compression pressure ratio and throttling losses; hence, multi-stage compression can improve this system. Multi-stage vapour compression systems can be classified as compound or cascade systems and consist of two independently operated single-stage refrigeration systems [8]. Under a standard condition, Cao et al. [9] found energy and economic benefits for an HFC-152a two-stage heat pump system with a flash tank for heating water to temperatures as high as 95 °C. Mateu-Royo et al. [10] considered several environmentally friendly fluids in different two-stage configurations and found that at higher temperature lifts, an HFO-1336mzz(Z) two-stage cycle with an internal heat exchanger (IHX) provides adequate values of volumetric heating capacity and energy performance.

Furthermore, the interest in higher performance cascade system operation is growing because it can provide practical benefits, such as the use of a variety of combinations of refrigerants and lubricant oils, and the prevention of liquid backflow caused by a cold start [11]. Arpagaus et al. [12] reviewed various architectures for multi-temperature heat pumps and found that cascade cycles result in higher energy performance than other configurations. Yang et al. [13] have observed that a theoretical HFC-152a/CO_2 (high and low stages) in the moderate HTHP cascade can be advantageous for COP and exergy efficiency in comparison with a basic cycle under a standard condition. Wallerand et al. [14] highlighted that cascade cycles allow a wider temperature range and lift because of the possibility of having working fluids switch with applications in waste heat recovery. Bamigbetan et al. [15] included the HTHP cascade system among those with a potential for improving energy performance.

The search for the best refrigerant pair for cascade systems is critical, especially for one that can be used under extreme conditions, such as those shown by the HTHP applications. Averfalk et al. [3] concluded that appropriately designed HTHPs that consider climate-friendly refrigerants can present comparable performance with sytems that use hydrofluorocarbons (HFCs).
Critical temperature is one of the most important parameters for determining the most suitable refrigerant for the HTHP. Fukuda et al. [16] indicated that the theoretical HTHP COP is maximised when operating at a condensation temperature of approximately 20 K below the working fluid critical temperature.

Therefore, the HTHP industry is currently searching for refrigerants with low global warming potential (GWP), and capable of operating at higher heat production temperatures and wider

temperature lifts. First, a few mixtures were proposed and investigated. Pan et al. [17] found that the zeotropic mixture HFC-245fa/HC-600 is considerably better than pure fluid HFC-245fa. Oue and Okada [18] investigated the HTHP performance using other zeotropic HFC mixtures. Some prototypal mixtures (with unknown compositions) have been proposed. Yu et al. [19] proposed the use of MF-1 to reach temperatures as high as 120 °C. Additionally, Ma et al. [20] investigated a water-source HTHP cascade using BY-3(A&B) and HFC-245fa for the high and low-stage cycles, respectively. Using BY-4, Xiaohui et al. [21] demonstrated the significant influence of evaporating temperature and temperature lift on energy performance.

Besides natural refrigerants [15], the low GWP synthetic alternatives are currently being developed as part of the fourth-generation refrigerants [22]. For the moment, the only synthetic fluids considered for the HTHPs are hydrofluoroolefins (HFOs) HFO-1234ze(E) and its isomer HFO-1234ze(Z) [16]. Kondou and Koyama [11] considered a theoretical multi-stage cascade for the moderate HTHP under a standard condition. A three-stage extraction cycle with HFO-1234ze(E), HFO-1234ze(Z), and HFC-365mfc (for low, medium, and high stages, respectively) achieved the highest efficiency. According to Longo et al. [23], HFO-1234ze(Z) exhibits a higher heat transfer coefficient than those of refrigerants used today in heat pump applications. Moreover, its frictional pressure drop is similar to that of isobutane. Wu et al. [24] proposed a hybrid source cascade heat pump using HFO-1234ze(Z) and CO_2. The energy efficiency improvement reached 27.2% while operating at a condensing temperature of 100 °C. Similarly, Yu et al. [19] found an optimal pressure that can maximise COP.

Thus, the selection of the intermediate pressure (as well as the superheating and sub-cooling degrees) is critical in the resulting energy performance of cascade vapour compression cycles. Kim and Kim [25] concluded that the high-stage (HS) condensing temperature determines the pressure ratio of an HFC-410A/HFC-134a cascade air-conditioning system. Qu et al. [26] developed a controller to set the intermediate, superheating, and evaporating temperatures of a cascade air source heat pump water heater by means of the compressor, electronic expansion valves, and evaporator fan of the low-stage (LS) cycle. Stavset et al. [27] compared various evaporating temperatures to identify the optimum operating condition for a propane/butane cascade system to heat water from 95 to 115 °C. The maximum improvement in COP reached approximately 60%. Baakeem et al. [28] optimised four variables to find maximum COP with different refrigerants. Although the maximum COP of 6.17 was obtained using ammonia, the maximum enhancement in COP in comparison with that of a basic cycle was 69.15% using HFC-404A. Yin et al. [29] proposed four cascade energy efficiency-oriented control strategies for heating, ventilating, and air-conditioning systems and improved the energy efficiency by as high as 5.8%.

Apart from operating conditions, the cascade basic construction can further be efficiently improved using additional elements. Zhang et al. [30] indicated that COP of multistage cycle industrial heat pumps, which are integrated with additional components, is better than those of conventional cycles. Liu et al. [31] considered an IHX in an experimental HTHP to validate

zeotropic mixtures and highlighted the critical importance of checking pinch points in heat exchangers. Llopis et al. [32] proved that the IHX can increase the energy performance of the cascade system although it decreases the heat transfer rate.

Cascade configurations could be considered a solution to the limited performance of HTHPs working at high-temperature lifts. However, the resulting performance depends on several specifications: (i) the refrigerant pair, (ii) appropriate operating parameters, and (iii) additional components. The proper selection and combination of these items can enhance the energy performance and operating limits at levels that simpler traditional configurations cannot achieve. A few cases of moderate HTHP systems with restricted temperature lifts have been studied to date, and any of these systems can cover higher temperatures, maximise COP, consider IHXs, or include new refrigerants with low GWP. Hence, to cover higher heat sink temperatures and temperature lifts operating at the maximum energy efficiency and reduce greenhouse gas emissions, this paper proposes and discusses the analyses of different low GWP refrigerant pairs (including recently developed HFOs) in the optimised HTHP cascades. Before the calculation of definitive results, the utilisation and influence of the additional IHXs in both cycles are assessed. Thereafter, a multiparameter optimisation algorithm has been employed to identify the optimum working condition, including the intermediate pressure and IHX effectiveness of both stage cycles. Finally, using the optimal settings for each refrigerant pair, the volumetric flow rate of both cycles at the compressor suction, the heating capacity and coefficient of performance parameters is presented, discussed, and compared with the HFC HTHP cascade.

2. HTHP cascade with IHX system

2.1. System architecture

As has been justified in the previous section, the highest energy performance in the HTHP with high-temperature lifts can be obtained using a cascade vapour compression system with the IHX in both stages. Figure 1 presents the resulting system architecture and an example of its operation in a pressure-enthalpy (Ph) diagram.

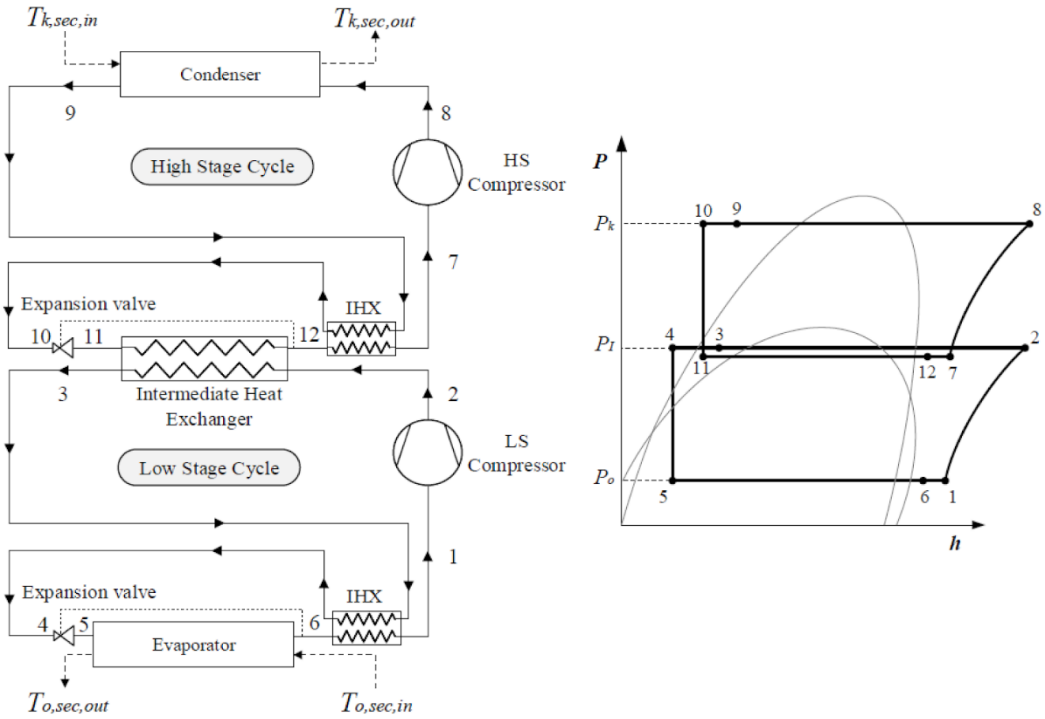

Fig. 1. Proposed system architecture and Ph diagram.

2.2. Equations for system modelling

The vapour suction temperature in both circuits is calculated using Eq. (1), considering the IHX effectiveness and establishing the superheating and sub-cooling degrees. Then, the enthalpy at the expansion device inlet is calculated considering the IHX heat balance given by Eq. (2).

$$\varepsilon_{IHX} = \frac{T_{suc} - T_{o,out}}{T_{k,out} - T_{o,out}} \tag{1}$$

$$h_{suc} - h_{o,out} = h_{x,in} - h_{k,out} \tag{2}$$

The heat absorbed by the LS cycle evaporator ($\dot{Q}_{o,LS}$) is proposed as input for the model in order to compare the compressor volumetric requirements for different refrigerant pairs; therefore, this heat transfer is considered constant. Then, the refrigerant mass flow rate of the LS cycle, $\dot{m}_{LS}$, is calculated using Eq. (3).

$$\dot{m}_{LS} = \frac{\dot{Q}_{o,LS}}{\left(h_{o,out,LS} - h_{o,in,LS}\right)} \tag{3}$$

The heating capacity of the LS cycle, $\dot{Q}_{k,LS}$, given by Eq. (4), is calculated by multiplying the mass flow rate by the enthalpy difference between the inlet and outlet in the condenser.

$$\dot{Q}_{k,LS} = \dot{m}_{LS}\left(h_{k,in,LS} - h_{k,out,LS}\right) \tag{4}$$

The same heating capacity above is assumed to be fully exchanged with the HS evaporator, and hence is equal to the cooling capacity of the HS cycle, $\dot{Q}_{o,HS}$, given by Eq. (5).

$$\dot{Q}_{o,HS} = \dot{Q}_{k,LS} \tag{5}$$

Therefore, the refrigerant mass flow rate of the HS cycle is calculated as shown in Eq. (6).

$$\dot{m}_{HS} = \frac{\dot{Q}_{o,HS}}{\left(h_{o,out,HS} - h_{o,in,HS}\right)} \tag{6}$$

Then, the heating production capacity, $\dot{Q}_{k,HS}$, given by Eq. (7), is calculated in the same manner as the heating capacity of the LS cycle.

$$\dot{Q}_{k,HS} = \dot{m}_{HS}\left(h_{k,in,HS} - h_{k,out,HS}\right) \tag{7}$$

Moreover, for both cycles, the required volumetric flow rate at the compressor suction ($\dot{V}_{suc}$), given by Eq. (8), is obtained from the mass flow rate, suction density, and volumetric efficiency.

$$\dot{V}_{suc} = \frac{\dot{m}}{\rho_{suc}\eta_{vol}} \tag{8}$$

The total compressor electric power consumption, $\dot{W}_C$, is expressed in Eq. (9) as the product of the mass flow rate and isentropic enthalpy increases at the compressor, divided by the isentropic and electromechanical efficiencies (assumed to be 0.95) for each stage.

$$\dot{W}_C = \frac{1}{\eta_{em}\left(\dot{m}_{HS}\frac{\Delta h_{is,c,HS}}{\eta_{is,HS}} + \dot{m}_{LS}\frac{\Delta h_{is,c,LS}}{\eta_{is,LS}}\right)} \tag{9}$$

The isentropic and volumetric efficiency of compressors is calculated using Pierre's correlations for "good" reciprocating compressors [1]. In this way, the volumetric efficiency, η_{vol}, is obtained from Eqs. (10) and (11).

$$\eta_{vol,HS} = k_1 \cdot \left(1 + k_s \cdot \frac{T_{suc,HS} - 18}{100}\right) \cdot \exp\left(k_2 \cdot \frac{P_k}{P_{I,HS}}\right) \tag{10}$$

$$\eta_{vol,LS} = k_1 \cdot \left(1 + k_s \cdot \frac{T_{suc,LS} - 18}{100}\right) \cdot \exp\left(k_2 \cdot \frac{P_{I,LS}}{P_o}\right) \tag{11}$$

where T_{suc} is the compressor suction temperature for both stages; $P_K/P_{I,HS}$ and $P_{I,LS}/P_o$ are the pressure ratios of the HS and LS cycle, respectively; k_1, k_s, and k_2 are Pierre's correlation constants with values of 1.04, 0.15, and −0.07, respectively.

Furthermore, the isentropic efficiency, η_{is}, is calculated following Pierre's correlation, as shown in Eqs. (12) and (13) [1]. The isentropic efficiencies are also used to calculate compressor discharge temperatures and condenser inlet enthalpies.

$$\left(\frac{\eta_{vol,HS}}{\eta_{is,HS}}\right) = \left(1 + k_e \cdot \frac{T_{suc,HS} - 18}{100}\right) \cdot \exp\left(a \cdot \frac{T_k}{T_{I,HS}} + b\right) \tag{12}$$

$$\left(\frac{\eta_{vol,LS}}{\eta_{is,LS}}\right) = \left(1 + k_e \cdot \frac{T_{suc,LS} - 18}{100}\right) \cdot \exp\left(a \cdot \frac{T_{I,LS}}{T_o} + b\right) \tag{13}$$

The constants are given by Pierre [1]: k_e, a, and b are −0.1, −2.40, and 2.88, respectively.

Finally, the coefficient of performance (COP) is calculated from the heating production capacity and total compressor electric power consumption, using Eq. (14).

$$COP = \frac{\dot{Q}_{k,HS}}{\dot{W}_C} \tag{14}$$

The total sub-cooling degree is assumed to be 10 K, and the temperature difference between the inlet ($T_{o,sec,in}$) and outlet ($T_{k,sec,out}$) condenser secondary fluid is 15 K. The total superheating degree is considered as15 K, and the temperature difference between the inlet ($T_{o,sec,in}$) and outlet ($T_{o,sec,out}$) evaporator secondary fluid is 10 K. For the condenser, evaporator, and intermediate heat exchanger, the pitch point is assumed to be 5 K. Moreover, an isenthalpic expansion process is considered, and the heat transfer to the surroundings and pressure drops are neglected. The refrigerant thermodynamic properties have been evaluated using the software applications Engineering Equation Solver (EES) [33] and REFPROP [34].

3. Refrigerants under consideration

In this HTHP cascade with the IHX system, only refrigerants with low GWP have been considered. Their positions (either at the HS or LS cycles) have been decided according to their critical temperature values, hence maximising the energy performance, as suggested in literature [16].

For the LS cycle, HFO-1234yf, HFO-1234ze(E), and the natural refrigerants, butane, isobutane, and propane, have been selected (Table 1). Both HFO-1234yf and HFO-1234ze(E) have been developed as HFC-134a low GWP replacements in air-conditioning and refrigeration systems [35] and are becoming relevant in different applications [36]. For the specific case of heat pump application, these refrigerants have been considered in hot water production by Nawaz et al. [37]. They also tested butane and propane (hydrocarbons) tested in heat pumps [38] at temperatures reaching 60 °C. Their critical temperature varies between 95 (HFO-1234yf) and 151.98 °C (both butane isomers). Their molecular structure implies that they are also flammable fluids [39] and

additional safety measures (such as additional ventilation or gas detectors) are required [40] in handling them. Nevertheless, for vapour compression systems embedded in a machinery room with access restricted to authorised personnel, there is no charge limitation for flammable refrigerants [41].

Table 1. Main characteristics of the LS refrigerants.

	HFO-1234yf	HFO-1234ze(E)	Butane (HC-600)	Isobutane (HC-600a)	Propane (HC-290)
ASHRAE safety class	A2L	A2L	A3	A3	A3
Molar mass [g·mol^{-1}]	114.04	114.04	58.12	58.12	44.10
P_{crit} [MPa]	3.38	3.63	3.80	3.80	4.25
T_{crit} [°C]	94.70	109.36	151.98	151.98	96.74
100 years GWP [42]	<1	<1	4	20	5
$\frac{\Delta h_{vap}}{c_{p,l} T_{crit}}$[a] [43]	0.25	0.29	0.32	0.30	0.29
Δh_{vap} [kJ·kg^{-1}][a]	141.2	163.1	356.3	323.3	326.7
Δh_{cond} [kJ·kg^{-1}][b]	50.53	93.4	276.5	233.3	132.8

[a] At the evaporation temperature of 30 °C

[b] At the condensation temperature of 90 °C

For the HS, working fluids with critical temperatures higher than those previously presented are required to condense in the subcritical operation (Table 2). Consequently, these critical temperatures vary between 155.5 (HCFO-1224yd(Z)) and 196.5 °C (pentane or n-pentane). At this instance, HCFO-1223zd(E) [44] and HFO-1336mzz(Z) [45] have been mostly considered in organic Rankine cycles; however, their use can be extended to the HTHPs because of their comparable temperature–pressure ranges. Refrigerant HCFO-1224yd(Z) has been recently developed as HFC-245fa substitute because of their considerably similar properties [46]. The refrigerant hydrocarbon pentane is the only flammable fluid considered in the HS cycle.

Table 2. Main characteristics of the HS refrigerants.

	HCFO-1233zd(E)	HFO-1336mzz(Z)	HCFO-1224yd(Z)	Pentane (R601)
ASHRAE safety class.	A1	A1	A1	A3
Molar mass [g mol^{-1}]	130.50	164.06	148.49	72.15
P_{crit} [MPa]	3.77	2.90	3.34	3.37
T_{crit} [°C]	165.60	171.27	155.54	196.54
100 years GWP [42]	<1	2	1	<1
$\frac{\Delta h_{vap}}{c_{p,l} T_{crit}}$[a] [43]	0.28	0.24	0.25	0.27
Δh_{vap} [kJ·kg^{-1}] [a]	154.2	136.3	128.8	313
Δh_{cond} [kJ·kg^{-1}] [b]	80.13	78.16	49.47	222.8

[a] At the evaporation temperature of 85 °C

[b] At the condensation temperature of 150 °C

In vapour compression systems with the IHX, the lower $\frac{\Delta h_{vap}}{c_{p,l} T_{crit}}$ ratio is, the higher the COP expected [43]. Hence, this ratio has been calculated for the refrigerants listed in Tables 1 and 2. Both HFO-1234yf and HFO-1336mzz(Z) show the best predicted IHX benefits for the LS and HS, followed by HFO-1234ze(E) and pentane, and HCFO-1224yd(Z). The constrained operating pressure model of Hermes et al. [47] suggests that COP increases with the use of propane and isobutane. Among the proposed fluids with low GWP, only HFO-1234yf and HFO-1234ze(E) have been experimentally tested in the IHX vapour compression systems and thereby confirmed noticeable COP improvement [48,49].

4. Internal Heat Exchanger Analysis

This section discusses the effect of the IHXs introduced in both cascade stages and the benefit provided in the overall system when the IHXs effectiveness is varied. The parameters analysed are the intermediate temperature, total COP, and LS and HS discharge temperatures. The resulting values are shown using a box-and-whisker plot format.

Firstly, the effectiveness of HS IHX over some parameters is considered, as shown in Fig. 2. The increase of this parameter decreases the intermediate temperature for the optimal COP and the discharge temperature of the LS cycle. Moreover, it increases total COP and HS discharge temperature. This is caused by reductions in the intermediate temperature for the higher effectiveness of the HS IHX. Hence, it decreases the LS pressure ratio, increases the HS pressure ratio as well as its discharge temperature at the same time. The result of this opposite evolution is the increment in total COP because the reduction in the LS pressure ratio is more relevant to the energy efficiency of the system. Therefore, the sub-cooling degree increments in the HS cycle increase the HS cooling capacity. Consequently, the intermediate temperature decreases for the absorbed heat. However, although the optimal HS IHX effectiveness should be unity, this parameter could be restricted by the remarkable HS discharge temperature increase.

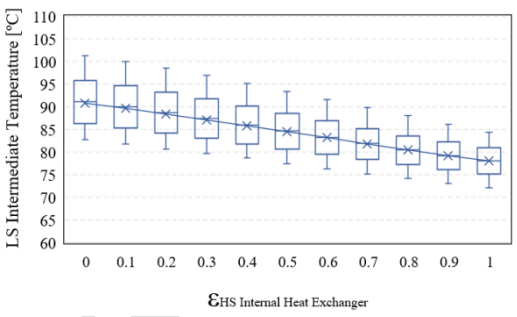

(a)

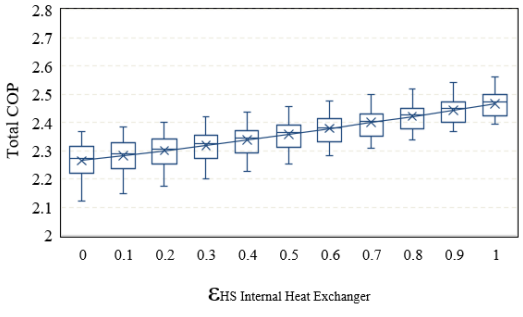

(b)

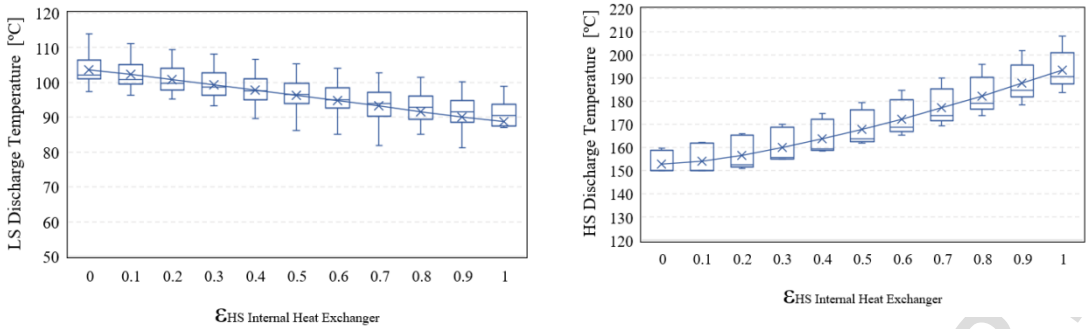

(c) (d)

Fig. 2. Variation of parameters at different HS IHX effectiveness: a) LS intermediate temperature, b) Total COP, c) LS discharge temperature, and d) HS discharge temperature.

Secondly, the effectiveness of the LS IHX on the same parameters above is considered, as presented in Fig. 3. With its increase, the intermediate temperature is increased, and total COP is increased at a proportion similar to that of the HS IHX effectiveness. Thereafter, it increases the HS discharge temperature to a lesser degree than that mentioned above. The LS discharge temperature increases because the greater LS pressure ratio keeps the total LS superheating degree constant. Based on these results, it can be concluded that the LS IHX effectiveness should attain the highest possible value if the limiting HS or LS discharge temperature value is not reached.

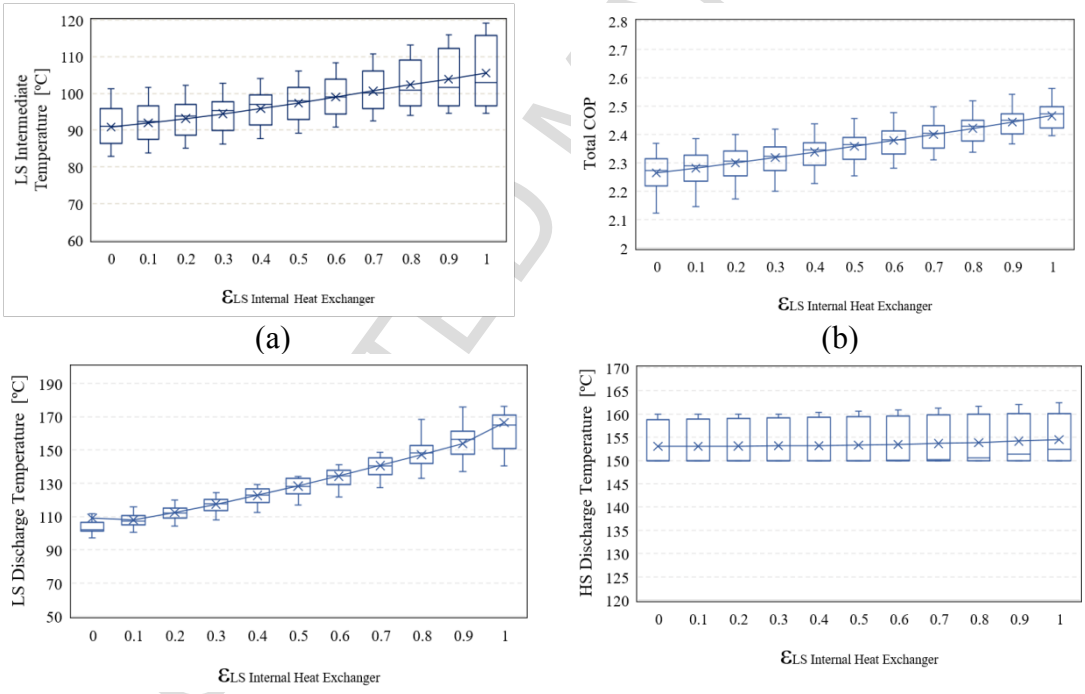

(a) (b)

(c) (d)

Fig. 3. Variation of different parameters at different LS IHX effectiveness: a) LS intermediate temperature, b) Total COP, c) LS discharge temperature, and d) HS discharge temperature.

5. Cascade optimisation and operating conditions

The intermediate temperature (the LS condenser temperature) is an input parameter of the cascade IHX model. Because it influences the energy performance of the entire system, this parameter

requires optimisation. The appropriate selection of the intermediate temperature can be difficult; therefore, several methods have been developed to find the optimum value.

Jeong and Smith [50] stated that the optimum intermediate temperature is obtained using the geometric mean of evaporation and condensation temperatures. Furthermore, Soltani et al. [51] concluded that the optimum intermediate temperature for two-stage refrigeration cycles notably differs from the geometric mean temperature. According to Di Nicola et al. [52], the optimum intermediate temperature in cascade cycles is influenced by the different pairs of working fluids.

Hence, this study utilises Powell's conjugate direction method to perform the optimisation of the system. The basic idea behind this method (integrated into the EES software) is to use a series of one-dimensional searches to locate the optimum, which is a function of several variables [53]. It varies the LS intermediate temperature and the effectiveness of the HS and LS IHXs to maximise COP, as shown in Fig. 4. Boundary conditions for the LS intermediate temperature are set to [0,175] °C, whereas those for the IHX effectiveness are [0,1]. The maximum HS discharge temperature is limited to 175 °C because the HFO fluids and polyolester lubricants can be degraded at temperatures above 180 °C [54,55]. As a result, because the HS discharge temperature is highly dependent on the effectiveness of the two IHX (demonstrated in section 4), this value can be limited and thereby restrict the condenser inlet enthalpy and pressure.

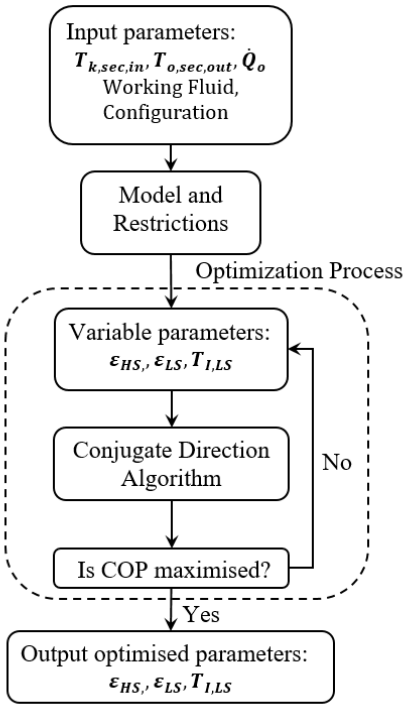

Fig. 4. Diagram of the optimisation process.

To simulate high-temperature applications, the heating production temperature ($T_{k,sec,out}$) remains constant at 145 °C. Thereafter, three waste heat temperatures ($T_{o,sec,in}$): 30, 45, and 60 °C, are considered to represent different situations of low-grade waste heat sources. These

temperatures are selected to achieve a notable temperature lift, with which cascade systems attain higher performance compared to single-stage systems.

6. Optimised configuration results

6.1. Results of the optimised configuration cascades

This section presents the output results of the optimised model for each refrigerant pair at the three waste heat temperatures (temperature lifts) proposed.

The optimised intermediate temperatures are presented in Fig. 5. Whereas HFO-1234yf, HFO-1234ze(E), and propane show intermediate temperatures in the LS cycle, between 90 and 100 °C, butane and isobutane achieve higher values because of their higher critical temperatures compared with those of other LS refrigerants. This advantage presented by butane and isobutane, based on their thermodynamic properties, is presented in the following discussions.

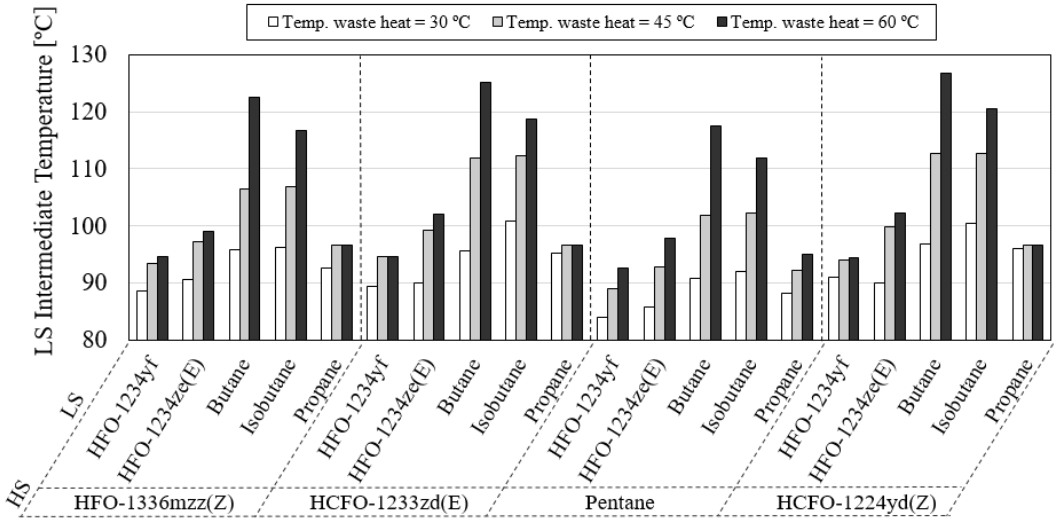

Fig 5. Intermediate Temperatures of the HTHP cascade system (at LS).

The optimisation algorithm suggests an LS IHX effectiveness value of 1 for all simulations, whereas the HS IHX effectiveness varies depending on the refrigerant pair, as shown in Fig. 6. The above is based on the lower temperature lift of the LS than that of the HS cycle. Thus, the selected LS IHX effectiveness could be the highest possible effectiveness that could be achieved without exceeding the discharge temperature limit. On the other hand, the HS IHX effectiveness, depends on the discharge temperature limit.

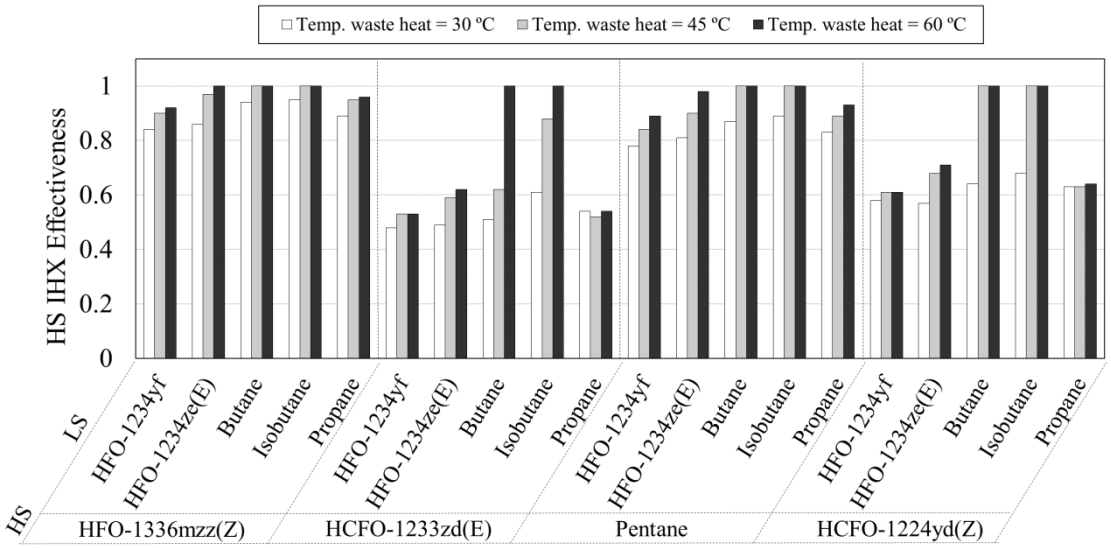

Fig 6. IHX Effectiveness of the HTHP cascade system (at LS).

The total compressor electric power consumption is presented in Fig. 7. In this case, all the LS refrigerants show similar behaviours regardless of the HS refrigerant. Butane and isobutane are the LS refrigerants that present the lowest consumptions, followed by propane, then hydrofluoroolefins.

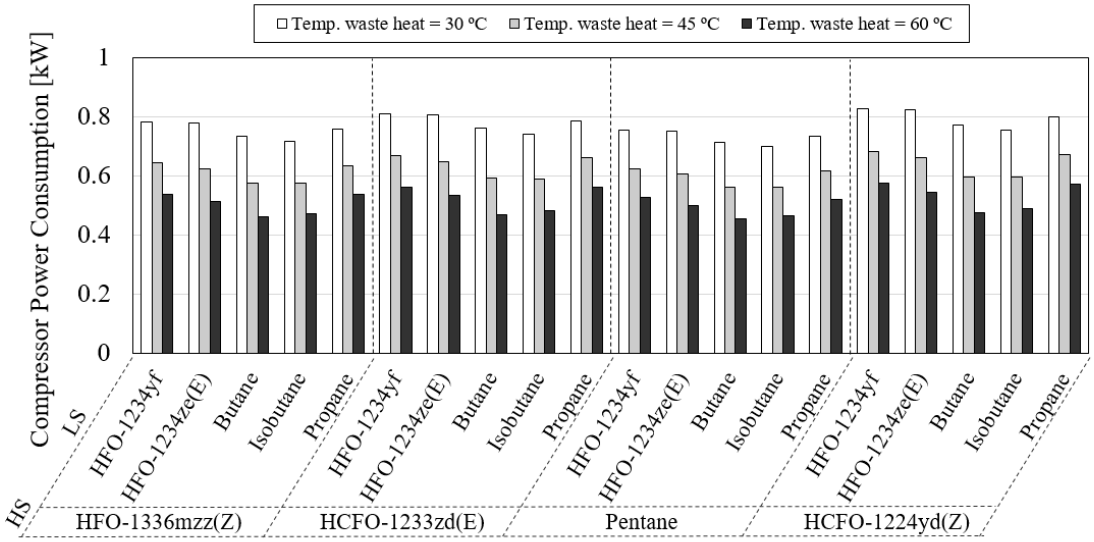

Fig 7. Total compressor electric power consumption of the HTHP cascade system.

To determine the most appropriate refrigerant pair, the refrigerant volumetric flow rates for the LS and HS cycles are shown in Fig. 8. The compressor size and installation are indicated by $\dot{V}_{suc}$; therefore, the higher $\dot{V}_{suc}$ is, the higher the installation cost. At the lowest waste heat temperature, the HS synthetic fluids combined with butane require comparable $\dot{V}_{suc,LS}$; pentane provides the lowest values when used with propane. At higher waste heat temperatures, $\dot{V}_{suc,LS}$ results are considerably reduced and become comparable among the four HS alternatives. The above conclusions similarly apply to $\dot{V}_{suc,HS}$. The refrigerant pairs that exhibit lower $\dot{V}_{suc,LS}$ result in a

higher $\dot{V}_{suc,HS}$, and vice versa. Because of this, the selection of the appropriate refrigerant pair requires additional comprehensive economic analyses of both stage components.

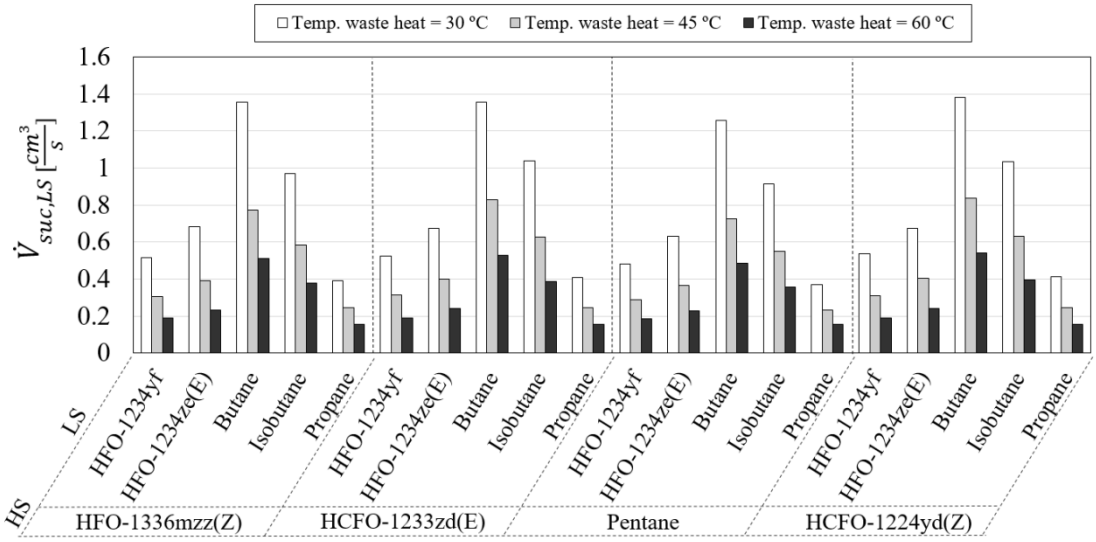

a)

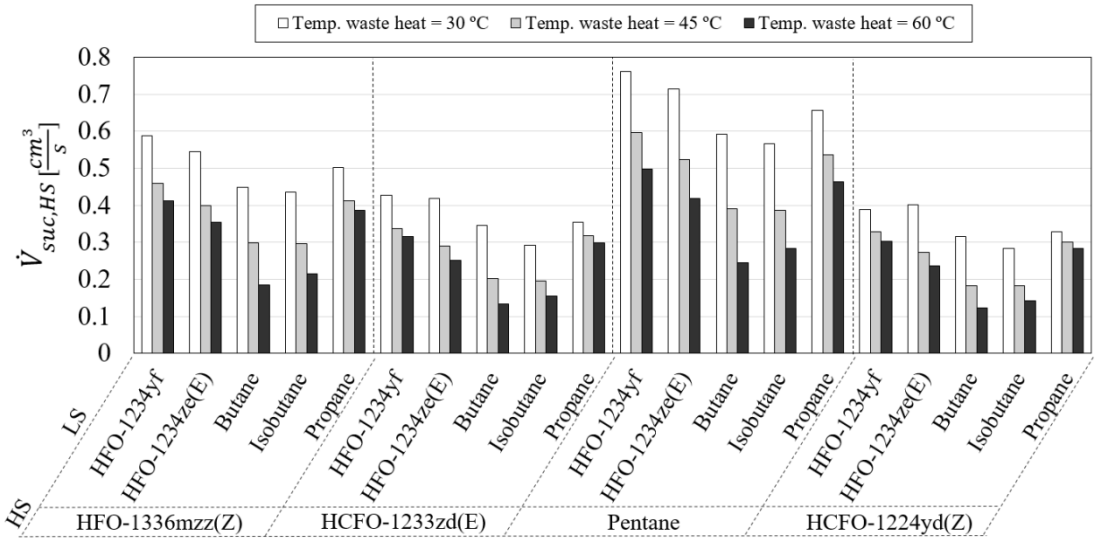

b)

Fig 8. Volumetric flow rate for the a) LS and b) HS compressor.

Figure 9 presents the results of the heating production capacity of the optimised HTHP cascade system. All the proposed refrigerant pairs provide comparable results; therefore, this parameter cannot be considered critical for system design. At the waste heat temperature of 30 °C, the maximum heating capacity is 1.79 kW for HCFO-1224yd(Z)/HFO-1234yf, and the minimum is 1.65 kW for pentane/isobutane. Besides, at the waste heat temperature of 60 °C, the resulting maximum heating capacity is 1.55 kW for HCFO-1224yd(Z)/propane, whereas the minimum is 1.42 kW for pentane/isobutane. Therefore, the variation at the same waste heat temperature does not exceed 7%.

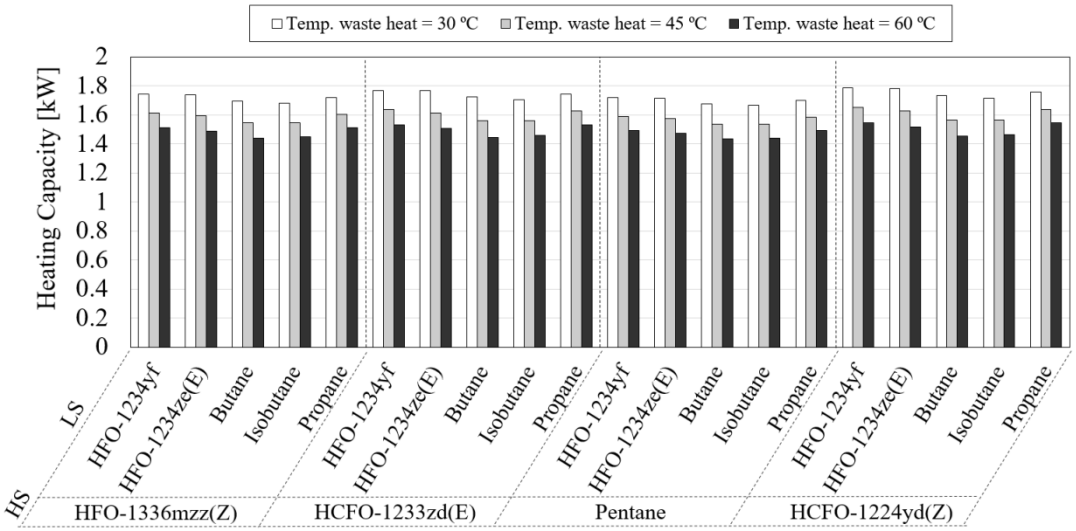

Fig 9. Heating capacity of the HTHP cascade system (at HS).

Finally, the global energy performance of the HTHP cascade system is represented by COP. The highest COP results for the three operating temperatures are obtained for butane in the LS cycle, followed by isobutane. The selected HS refrigerant has a smaller influence on COP; by using HFO-1336mzz(Z) and pentane, higher results are obtained. At the waste heat temperature of 30 °C, COP is 2.38 for pentane/isobutane, and the minimum is 2.16 for HCFO-1224yd(Z)/HFO-1234yf. Nevertheless, at the waste heat temperature of 60 °C, maximum COP is 3.15 for pentane/butane, and the minimum is 2.69 for HCFO-1224yd(Z)/HFO-1234yf.

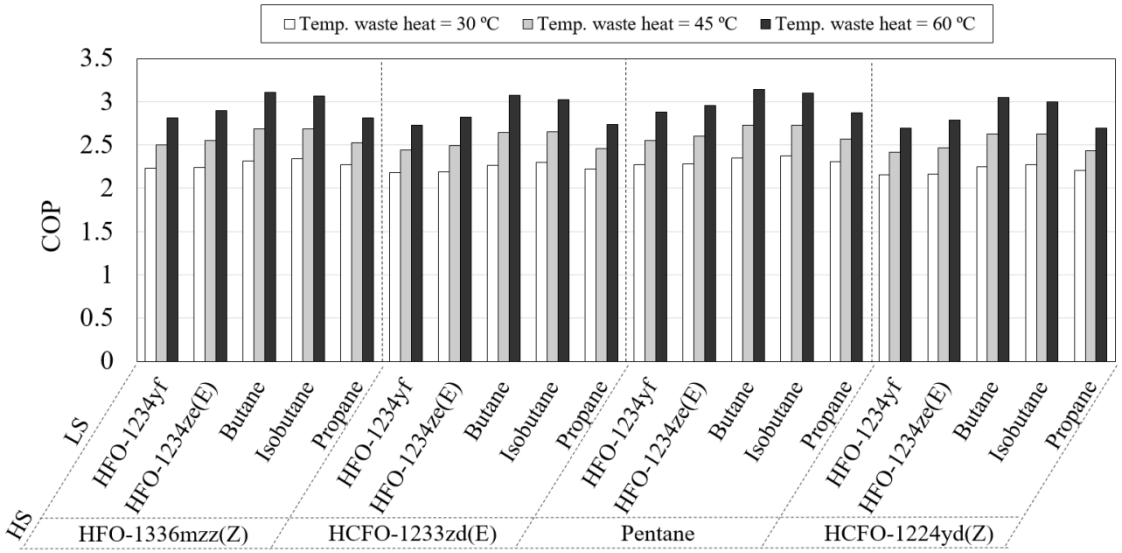

Fig. 10. Optimised COP for different refrigerant pairs and waste heat temperatures.

The optimised HTHP cascade system results depict that butane appears to be the more suitable fluid from a $\dot{V}_{suc,LS}$ and COP point of view, whereas HFO-1234yf can be the more appropriate fluid from the perspective of $\dot{V}_{suc,HS}$ and heating production capacity. Regarding the optimum HS refrigerant, relevant differences are only observed in parameter $\dot{V}_{suc,HS}$, with pentane exhibiting the highest values. For the rest of the studied parameters, slight differences can be

observed: HCFO-1224yd(Z) presents the highest results for $\dot{V}_{suc,LS}$ and heating capacity, whereas pentane exhibits the highest for COP.

6.2. Comparison with an HTHP cascade using third-generation refrigerants

This section compares Section 6.1 results with an HTHP cascade that uses typical third-generation refrigerants [22], which are considered as baseline. The aim is to check the benefits of these fourth-generation refrigerants in the optimised HTHP cascades. The third-generation refrigerants considered are the greenhouse gases HFC-245fa for the HS cycle and HFC-134a for the LS cycle. The improvement in COP is shown in the y-axis, whereas in Fig. 10.a), parameter $\dot{V}_{suc,HS}$ is selected for the x-axis; in Fig. 10.b), parameter $\dot{V}_{suc,LS}$ is considered. The LS refrigerant can be identified by its colour and the HS refrigerant by its symbol. Both are connected by a dashed line.

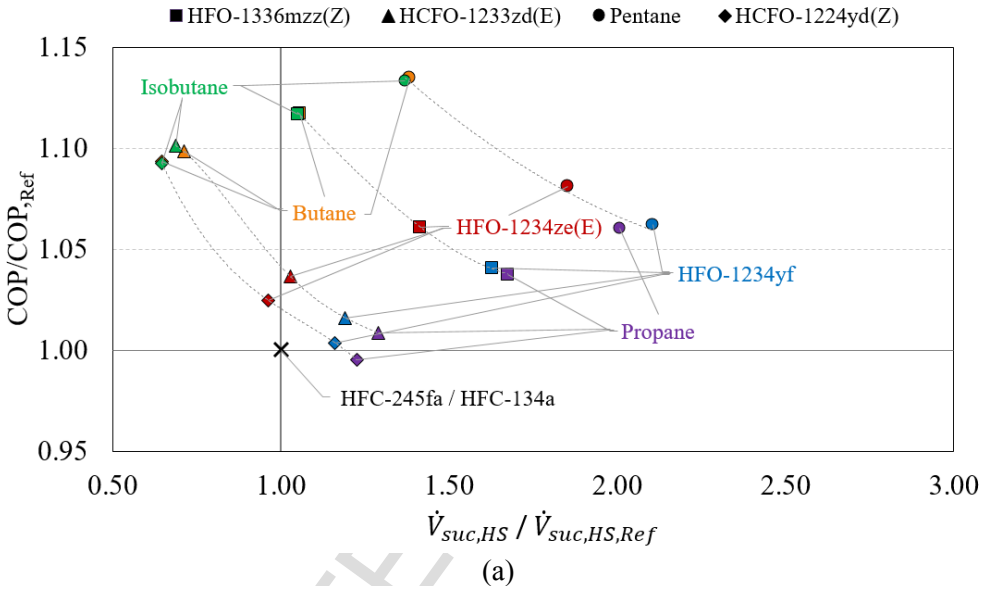

(a)

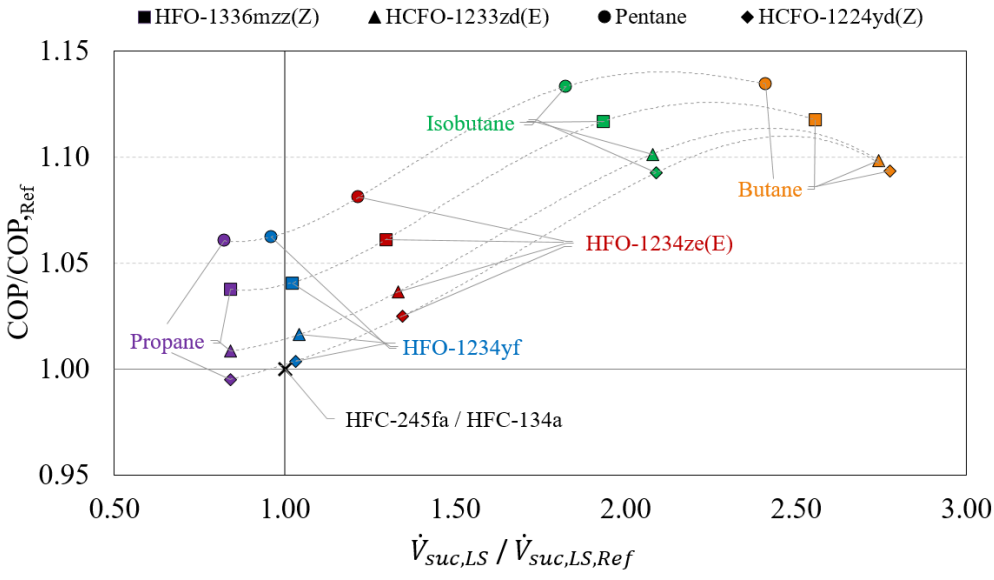

(b)

Fig. 11. Low GWP HTHP cascade system comparison with third-generation refrigerants considering a) $\dot{V}_{suc,HS}$ and b) $\dot{V}_{suc,LS}$.

All the new refrigerant pairs increase COP in comparison with HFC-245fa/HFC-134a cascade, except for propane and HFO-1234yf with HCFO-1224yd(Z), which show comparable results. The highest COP improvement (13%) is obtained using pentane with butane and isobutane. The results of $\dot{V}_{suc,HS}$ are more influenced by the refrigerant pair selection, and refrigerants with the highest reductions are HCFO-1224yd(Z) and HCFO-1233zd(E) with butane and isobutane. Moreover, propane is the only LS refrigerant that achieves a reduction in $\dot{V}_{suc,LS}$ (approximately 15%), whereas HFO-1234yf presents similar results with the baseline.

Pentane and HFO-1336mzz(Z) in the HS cycle result in the highest value of COP and $\dot{V}_{suc,HS}$. In contrast, COP improvement is lower when HCFO-1233zd(E) and HCFO-1224yd(Z) are considered, and $\dot{V}_{suc,HS}$ is similar or even lower. In terms of $\dot{V}_{suc,LS}$, pentane and HFO-1336mzz(Z) are more benefited than HCFO-1233zd(E) and HCFO-1224yd(Z) are. Furthermore, depending on the refrigerant in the LS cycle, the differences in $\dot{V}_{suc,LS}$ between pentane, HFO-1336mzz(Z) and HCFO-1233zd(E), and HCFO-1224yd(Z) become more significant. For instance, propane has a similar $\dot{V}_{suc,LS}$ as the rest of the HS refrigerants, whereas butane shows a higher difference in $\dot{V}_{suc,LS}$ between pentane, HFO-1336mzz(Z) and HCFO-1233zd(E), and HCFO-1224yd(Z).

7. Conclusions

The HTHPs are vapour compression system applications that can work with high-temperature lift operations. The cascade configuration can allow an energy-efficient operation under these conditions. This study simulates and optimises different cascade configurations that consider the IHX in both cycles and using only refrigerants with low GWP in order to design an HTHP for high-temperature lifts with the lowest greenhouse gas emissions. Moreover, the heat production temperatures considered are higher than those previously reported in literature for cascade configurations.

Firstly, only synthetic and natural refrigerants with a GWP approximating unity have been considered. The LS candidate refrigerants are HFO-1234yf, HFO-1234ze(E), butane (HC-600), isobutane (HC-600a), and propane (HC-290); the HS candidate refrigerants are HCFO-1233zd(E), HFO-1336mzz(Z), HCFO-1224yd(Z), and pentane (HC-601). Their positions have been selected according to the critical temperature; hence, the optimum operating temperature range. All the LS refrigerants are flammable (HFO-1234yf and HFO-1234ze(E) are classified with low flammability), whereas the HS refrigerants are considered safe, except for pentane.

Secondly, the influence of the effectiveness of the LS and HS IHXs on several parameters has been studied. When the effectiveness is increased for both IHXs, total COP increases, and the intermediate pressure decreases to a comparable extent. A higher HS IHX effectiveness increases

the HS discharge temperature, but decreases that of the LS. Otherwise, the LS IHX effectiveness has a relatively low impact on the HS discharge temperature, but notably increases that of the LS.

Finally, an optimisation of the HTHP cascade system has been implemented for all refrigerant pairs. An algorithm maximises COP, which varies the intermediate temperature of the LS and the effectiveness of both IHXs. As for the optimised HTHP cascade results, butane and isobutane appear to be the more convenient LS refrigerants from the $\dot{V}_{suc,LS}$ and COP point of view, whereas propane and HFO-1234yf appear to be the more appropriate option in considering $\dot{V}_{suc,LS}$ and heating capacity. The highest energy performance of the system is achieved using pentane and HFO-1336mzz(Z) in the HS cycle, whereas HCFO-1233zd(E) and HCFO-1224yd(Z) provided a slight improvement in COP with a similar or even lower $\dot{V}_{suc,HS}$. The maximum resulting COP is 3.15 using pentane/butane, which results to a 13% improvement compared with that of the HFC-245fa/HFC-134a HTHP cascade (third-generation refrigerants). However, if a low flammable solution is required, the HFO-1336mzz(Z)/HFO-1234ze(E) is the option that presents a higher performance. A few low-GWP pairs can compete with this non-environmentally friendly cascade in terms of $\dot{V}_{suc,LS}$ and $\dot{V}_{suc,HS}$, but most of them present higher energy performances, and thereby result to lower greenhouse gas emissions.

Acknowledgements

The authors acknowledge the financial support of the Spanish Government under the ENE2015-70610-R and RTC-2015-4193-3 projects, and grant FJCI-2016-28324. Furthermore, the authors acknowledge the University Jaume I of Spain for their financial support under project P1-1B2015-38.

References

[1] Granryd E, Ekroth I, Lundqvist P, Melinder A, Palm B, Rohlin P. Refrigeration Engineering. K Tek Högskolan 1999.

[2] Panayiotou GP, Georgiou G, Aresti L, Argyrou M, Agathokleous R, Tsamos KM, et al. Preliminary assessment of waste heat potential in major European industries. Energy Procedia 2017;123:335–45. doi:10.1016/J.EGYPRO.2017.07.263.

[3] Averfalk H, Ingvarsson P, Persson U, Gong M, Werner S. Large heat pumps in Swedish district heating systems. Renew Sustain Energy Rev 2017;79:1275–84. doi:10.1016/j.rser.2017.05.135.

[4] Seck GS, Guerassimoff G, Maïzi N. Heat recovery with heat pumps in non-energy intensive industry: A detailed bottom-up model analysis in the French food & drink industry. Appl Energy 2013;111:489–504. doi:10.1016/j.apenergy.2013.05.035.

[5] Arpagaus C, Bless F, Uhlmann M, Schiffmann J, Bertsch SS. High temperature heat pumps: Market overview, state of the art, research status, refrigerants, and application potentials. Energy 2018;152:985–1010. doi:10.1016/J.ENERGY.2018.03.166.

[6] Chamoun M, Rulliere R, Haberschill P, Peureux J-L. Experimental and numerical investigations of a new high temperature heat pump for industrial heat recovery using water as refrigerant. Int J Refrig 2014;44:177–88. doi:10.1016/j.ijrefrig.2014.04.019.

[7] Zhao Z, Xing Z, Hou F, Tian Y, Jiang S. Theoretical and experimental investigation of a novel high temperature heat pump system for recovering heat from refrigeration system. Appl Therm Eng 2016;107:758–67. doi:10.1016/j.applthermaleng.2016.07.047.

[8] Chua KJ, Chou SK, Yang WM. Advances in heat pump systems: A review. Appl Energy 2010;87:3611–24. doi:10.1016/j.apenergy.2010.06.014.

[9] Cao X-Q, Yang W-W, Zhou F, He Y-L. Performance analysis of different high-temperature heat pump systems for low-grade waste heat recovery. Appl Therm Eng 2014;71:291–300. doi:10.1016/j.applthermaleng.2014.06.049.

[10] Mateu-Royo C, Navarro-Esbrí J, Mota-Babiloni A, Amat-Albuixech M, Molés F. Theoretical evaluation of different high-temperature heat pump configurations for low-grade waste heat recovery. Int J Refrig 2018. doi:10.1016/j.ijrefrig.2018.04.017.

[11] Kondou C, Koyama S. Thermodynamic assessment of high-temperature heat pumps using low-GWP HFO refrigerants for heat recovery. Int J Refrig 2015;53:126–41. doi:10.1016/j.ijrefrig.2014.09.018.

[12] Arpagaus C, Bless F, Schiffmann J, Bertsch SS. Multi-temperature heat pumps: A literature review. Int J Refrig 2016;69:437–65. doi:10.1016/j.ijrefrig.2016.05.014.

[13] Yang W wei, Cao X qi, He Y ling, Yan F yu. Theoretical study of a high-temperature heat pump system composed of a CO2 transcritical heat pump cycle and a R152a subcritical heat pump cycle. Appl Therm Eng 2017;120:228–38. doi:10.1016/j.applthermaleng.2017.03.098.

[14] Wallerand AS, Kermani M, Kantor I, Maréchal F. Optimal heat pump integration in industrial processes. Appl Energy 2018;219:68–92. doi:10.1016/j.apenergy.2018.02.114.

[15] Bamigbetan O, Eikevik TM, Nekså P, Bantle M. Review of vapour compression heat pumps for high temperature heating using natural working fluids. Int J Refrig 2017;80:197–211. doi:10.1016/j.ijrefrig.2017.04.021.

[16] Fukuda S, Kondou C, Takata N, Koyama S. Low GWP refrigerants R1234ze(E) and R1234ze(Z) for high temperature heat pumps. Int J Refrig 2014;40:161–73. doi:10.1016/j.ijrefrig.2013.10.014.

[17] Pan L, Wang H, Chen Q, Chen C. Theoretical and experimental study on several refrigerants of moderately high temperature heat pump. Appl Therm Eng 2011;31:1886–93. doi:10.1016/j.applthermaleng.2011.02.035.

[18] Oue T, Okada K. Air-sourced 90??C hot water supplying heat pump, “hEM-90A.” R D Res Dev Kobe Steel Eng Reports 2013;63:47–50.

[19] Yu X, Zhang Y, Kong L, Zhang Y. Thermodynamic analysis and parameter estimation of a high-temperature industrial heat pump using a new binary mixture. Appl Therm Eng 2018;131:715–23. doi:10.1016/j.applthermaleng.2017.12.039.

[20] Ma X, Zhang Y, Li X, Zou H, Deng N, Nie J, et al. Experimental study for a high efficiency cascade heat pump water heater system using a new near-zeotropic refrigerant mixture. Appl Therm Eng 2017. doi:10.1016/J.APPLTHERMALENG.2017.12.124.

[21] Yu X, Zhang Y, Deng N, Chen C, Ma L, Dong L, et al. Experimental performance of high temperature heat pump with near-azeotropic refrigerant mixture. Energy Build 2014;78:43–9. doi:10.1016/j.enbuild.2013.12.065.

[22] Calm JM. The next generation of refrigerants – Historical review, considerations, and outlook. Int J Refrig 2008;31:1123–33. doi:10.1016/J.IJREFRIG.2008.01.013.

[23] Longo GA, Zilio C, Righetti G, Brown JS. Experimental assessment of the low GWP

refrigerant HFO-1234ze(Z) for high temperature heat pumps. Exp Therm Fluid Sci 2014;57:293–300. doi:10.1016/j.expthermflusci.2014.05.004.

[24] Wu D, Hu B, Wang RZ. Performance simulation and exergy analysis of a hybrid source heat pump system with low GWP refrigerants. Renew Energy 2018;116:775–85. doi:10.1016/j.renene.2017.10.024.

[25] Kim DH, Kim MS. The effect of water temperature lift on the performance of cascade heat pump system. Appl Therm Eng 2014;67:273–82. doi:10.1016/j.applthermaleng.2014.03.036.

[26] Qu M, Fan Y, Chen J, Li T, Li Z, Li H. Experimental study of a control strategy for a cascade air source heat pump water heater. Appl Therm Eng 2017;110:835–43. doi:10.1016/j.applthermaleng.2016.08.176.

[27] Stavset O, Banasiak K, Hafner A. Analysis of high temperature heat pumps applying natural working fluids. 11th IIR Gustav Lorentzen Conf. Nat. Refrig. Nat. Refrig. Environ. Prot. GL 2014, 2014.

[28] Baakeem SS, Orfi J, Alabdulkarem A. Optimization of a multistage vapor-compression refrigeration system for various refrigerants. Appl Therm Eng 2018;136:84–96. doi:10.1016/J.APPLTHERMALENG.2018.02.071.

[29] Yin X, Wang X, Li S, Cai W. Energy-efficiency-oriented cascade control for vapor compression refrigeration cycle systems. Energy 2016;116:1006–19. doi:10.1016/j.energy.2016.10.059.

[30] Zhang J, Zhang H-H, He Y-L, Tao W-Q. A comprehensive review on advances and applications of industrial heat pumps based on the practices in China. Appl Energy 2016;178:800–25. doi:10.1016/j.apenergy.2016.06.049.

[31] Liu Z, Zhao L, Zhao X, Li H. The occurrence of pinch point and its effects on the performance of high temperature heat pump. Appl Energy 2012;97:869–75. doi:10.1016/j.apenergy.2011.12.061.

[32] Llopis R, Sanz-Kock C, Cabello R, Sánchez D, Nebot-Andrés L, Catalán-Gil J. Effects caused by the internal heat exchanger at the low temperature cycle in a cascade refrigeration plant. Appl Therm Eng 2016;103:1077–86. doi:10.1016/j.applthermaleng.2016.04.075.

[33] Klein S. Engineering Equation Solver (EES) V10.2. Fchart Software, Madison, USA WwwFchartCom 2006.

[34] Lemmon EW, Huber ML, McLinden MO. NIST Standard Reference Database 23. Ref Fluid Thermodyn Transp Prop (REFPROP), Version 91 2013.

[35] Mendoza-Miranda JMM, Mota-Babiloni A, Ramírez-Minguela JJJ, Muñoz-Carpio VDD, Carrera-Rodríguez M, Navarro-Esbrí J, et al. Comparative evaluation of R1234yf, R1234ze(E) and R450A as alternatives to R134a in a variable speed reciprocating compressor. Energy 2016;114:753–66. doi:10.1016/j.energy.2016.08.050.

[36] Mota-Babiloni A, Makhnatch P, Khodabandeh R. Recent investigations in HFCs substitution with lower GWP synthetic alternatives: Focus on energetic performance and environmental impact. Int J Refrig 2017;82. doi:10.1016/j.ijrefrig.2017.06.026.

[37] Nawaz K, Shen B, Elatar A, Baxter V, Abdelaziz O. R1234yf and R1234ze(E) as low-GWP refrigerants for residential heat pump water heaters. Int J Refrig 2017;82:348–65. doi:10.1016/j.ijrefrig.2017.06.031.

[38] Nawaz K, Shen B, Elatar A, Baxter V, Abdelaziz O. R290 (propane) and R600a

(isobutane) as natural refrigerants for residential heat pump water heaters. Appl Therm Eng 2017;127:870–83. doi:10.1016/j.applthermaleng.2017.08.080.

[39] McLinden MO, Brown JS, Brignoli R, Kazakov AF, Domanski PA. Limited options for low-global-warming-potential refrigerants. Nat Commun 2017;8. doi:10.1038/ncomms14476.

[40] EN 378-3:2017. Refrigerating systems and heat pumps. Safety and environmental requirements. Installation site and personal protection. Brussels, Belgium: 2017.

[41] EN 378-1:2017. Refrigerating systems and heat pumps. Safety and environmental requirements. Basic requirements, definitions, classification and selection criteria. Brussels, Belgium: 2017.

[42] ASHRAE. ASHRAE Handbook Fundamentals. Am Soc Heating, Refrig Air-Conditioning Eng 2017.

[43] Klein SA, Reindl DT, Brownell K. Refrigeration system performance using liquid-suction heat exchangers. Int J Refrig 2000;23:588–96. doi:10.1016/S0140-7007(00)00008-6.

[44] Molés F, Navarro-Esbrí J, Peris B, Mota-Babiloni A. Experimental evaluation of HCFO-1233zd-E as HFC-245fa replacement in an Organic Rankine Cycle system for low temperature heat sources. Appl Therm Eng 2016;98. doi:10.1016/j.applthermaleng.2016.01.011.

[45] Navarro-Esbrí J, Molés F, Peris B, Mota-Babiloni A, Kontomaris K. Experimental study of an Organic Rankine Cycle with HFO-1336mzz-Z as a low global warming potential working fluid for micro-scale low temperature applications. Energy 2017;133. doi:10.1016/j.energy.2017.05.092.

[46] AGC Chemicals. AMOLEA® 1224yd, Technical information. ASAHI Glas Co 2017:1–18.

[47] Hermes CJL. Alternative evaluation of liquid-to-suction heat exchange in the refrigeration cycle. Int J Refrig 2013;36:2119–27. doi:10.1016/J.IJREFRIG.2013.06.007.

[48] Cho H, Lee H, Park C. Performance characteristics of an automobile air conditioning system with internal heat exchanger using refrigerant R1234yf. Appl Therm Eng 2013;61:563–9. doi:10.1016/j.applthermaleng.2013.08.030.

[49] Mota-Babiloni A, Navarro-Esbrí J, Barragán-Cervera A, Molés F, Peris B. Drop-in analysis of an internal heat exchanger in a vapour compression system using R1234ze(E) and R450A as alternatives for R134a. Energy 2015;90. doi:10.1016/j.energy.2015.06.133.

[50] Jeong S, Smith JL. Optimum temperature staging of cryogenic refrigeration system. Cryogenics (Guildf) 1994;34:929–33. doi:10.1016/0011-2275(94)90078-7.

[51] Soltani R, Dincer I, Rosen MA. Comparative performance evaluation of cascaded air-source hydronic heat pumps. Energy Convers Manag 2015;89:577–87. doi:10.1016/j.enconman.2014.10.006.

[52] Di Nicola G, Giuliani G, Polonara F, Stryjek R. Blends of carbon dioxide and HFCs as working fluids for the low-temperature circuit in cascade refrigerating systems. Int J Refrig 2005;28:130–40. doi:10.1016/j.ijrefrig.2004.06.014.

[53] Powell MJD. An efficient method for finding the minimum of a function of several variables without calculating derivatives. Comput J 1964. doi:10.1093/comjnl/7.2.155.

[54] Kontomaris K. A zero-ODP, low GWP working fluid for high temperature heating and

power generation from low temperature heat: DR-2. Proc JRAIA Int Symp 2012 2012:212–6.

[55] Navarro-Esbrí J, Molés F, Peris B, Mota-Babiloni A. Small scale orc design for a cogeneration solar biomass suported application. 3rd Int Semin ORC Power Syst Oct 12-14, 2015, Brussels, Belgium 2015.